

THE Z PULSED POWER DRIVER SINCE REFURBISHMENT

M.E. Savage, D.S. Artery, B.W. Atherton, D.E. Bliss, P.A. Corcoran, M. E. Cuneo, J.P. Davis, C.A. Hall, M. Herrmann, M. Jones, M.D. Knudson, K.R. LeChien, R.J. Leeper, G.T. Leifeste, R.W. Lemke, F.W. Long, M.R. Lopez, M.K. Matzen, G.R. McKee, A.C. Owen, J.L. Porter, D.V. Rose, B.S. Stoltzfus, K.W. Struve, W.A. Stygar, R.D. Thomas, T.C. Wagoner, P.E. Wakeland, D.R. Welch, J.R. Woodworth

Sandia National Laboratories[§], Albuquerque, New Mexico, USA 87185

Abstract

Z is a multi-terawatt high current driver used to generate high energy density physics conditions. In September of 2007, the Z pulser resumed operation after a one-year shutdown for the Z refurbishment (ZR) project. The refurbishment project raised the stored energy and replaced most of the system components. Since then, the machine has been used for more than 300 high energy experiments, with the first year primarily devoted to developing full operational capability. The Z system delivers currents up to 26 MA, to vacuum loads of \sim 2.5 nH initial inductance inside a 15 cm diameter. The rise time (10%-90%) of the current is 85 nanoseconds or less into a fixed inductor. Z is now operated at an average rate of four experiments per week, generating a variety of high energy density physics conditions. Imploding plasma configurations generate megajoules of soft X-radiation from the stagnating z-pinch plasma. Z is also used for its high current capability (>20 MA) in cm and smaller width conductors, generating megagauss magnetic fields and the resulting high pressures. The high pressures are used for material equation of state measurements, and for basic science experiments. In addition to increasing the load current and energy capability during the rebuild, there have also been further improvements to the pulsed power systems since the rebuild to improve performance and reliability. Major improvements have been made to the diagnostics and waveform data acquisition systems. In this presentation we summarize the changes made during the refurbishment. We will describe the performance of the Z system, including reliability and jitter of the pulsed power system. We will note new capabilities, and describe the more recent improvements to the machine and diagnostics. We will also describe some of the experimental campaigns, highlighting achievements with megagauss magnetic field generation.

[§] *Sandia is a multiprogram laboratory operated by Sandia Corporation, a Lockheed Martin Company, for the United States Department of Energy's National Nuclear Security Administration under contract DE-AC04-94AL85000.*

Introduction

The Z energy storage system stores 28 megajoules at the maximum rated 100 kV charge voltage. At a charge voltage of 80 kV, where the system is normally operated, the Marx generators store 18 megajoules, and the pulse forming system generates a forward wave with a peak power of 82 terawatts, peak amplitude of 4 megavolts, and a source impedance of 0.18Ω . The energy contained in the forward wave is 6.9 megajoules at 80 kV Marx charge, creating a load current more than 27 megamperes into a fixed inductor, in the nominal 15 nanohenry (total) vacuum power feed system. Typically, even solid steel conductors move appreciably on a 100-nanosecond time scale when the linear current density exceeds one megampere per millimeter, and so most load configurations experience noticeable inductance increase. This inductance increase tends to limit the peak current. For imploding plasma (milligram) loads, where it is desirable to convert magnetic energy to radiation, the load current drops precipitously (as expected, and desired) when the imploding liner reaches high velocity. From the 82-terawatt forward going power pulse, X-radiation powers up to 320 terawatts have been recorded. Magnetic fields up to 1200 Tesla driving partially solid flyer plates have been verified with hydrodynamic simulations.

The Z pulsed power system is designed to supply large currents (with 85 nanosecond 10%-90% rise time) to high energy density physics experiments in vacuum, at a rate of one experiment per day. Z is used to drive imploding plasma loads (e.g., z-pinches), and dynamic material property loads for characterizing materials under high pressures. The Z pulsed power system is physically large, comprised of an oil-insulated DC-charged section, a deionized water insulated pulse charged section, and a vacuum magnetically insulated final feed and load. The Z tank outer diameter is 33m. The volume of mineral-based transformer oil is 3.2 million liters. The volume of deionized water is approximately one million liters. The refurbished Z driver is the highest current reusable laboratory pulsed source in existence. The Z system is based on evolutionary development of fast (sub-microsecond) multi-terawatt pulsed power systems for driving high current particle beams, and magnetically driven implosions. Such systems have been

built for inertial confinement fusion research, and radiation effects studies; recently there has been considerable interest in dynamic material property studies at megabar pressures, and in studies of astrophysical plasmas. High current drivers are suitable for addressing aspects of each of those areas.

High current drivers are relatively efficient sources of high energy density conditions. For example, from the 18 megajoules stored at 80 kV Marx charge voltage, Z has created 2.4 megajoules of soft X-rays (up to 1 keV) from nested tungsten wire arrays. This corresponds to an energy efficiency of 13% from stored energy to fast pulsed soft X-radiation. Figure 1 shows a view of the Z pulsed power system.

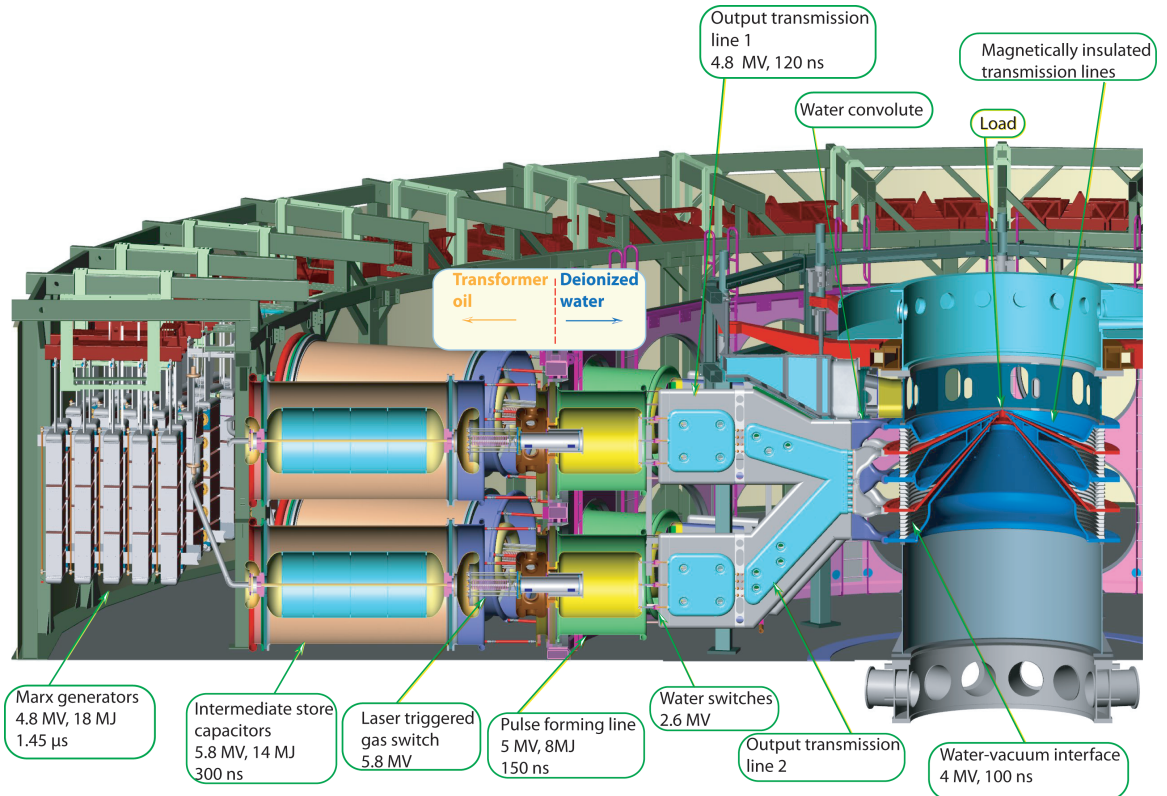


Figure 1. Cross-sectional view of the Z pulsed power system. Typical peak voltages at ± 80 kV Marx charge, stored energies, and discharge times are shown. For switches, typical peak terminal voltages are shown. The outer tank diameter is 33m.

As a user facility, flexibility is crucial to the vitality of the program. For imploding plasma loads, minimizing the time to peak current is important for load

stability issues [1-3]. Magnetically driven flyer plate experiments [4] also require relatively short current rise times because of magnetic field penetration concerns. On the other hand, isentropic compression experiments [5] require longer rise times, to avoid shock formation in the millimeter thickness samples used. For this reason, the modular nature of Z is valuable. Each of the 36 modules of Z can be configured and timed independently. Avoiding shocks in material samples depends critically on the ability to shape the current pulse accurately.

Pulsed power system

The initial pulse compression element in Z is an array of 36 Marx generators [6]. Each Marx generator consists of 30 pairs of $2.6\ \mu\text{F}$ capacitors coupled with midplane triggered, field distortion switches. The upgraded Z Marx generators store $515\ \text{kJ}$ apiece at $\pm 80\ \text{kV}$ charge voltage. Each Marx generator's erected capacitance is $45\ \text{nF}$, has an equivalent series inductance of $14\ \mu\text{H}$, and charges the next pulse forming stage in $1.45\ \mu\text{s}$. The output time of the 36 Marxes has an eight nanosecond one standard deviation; at the same time the probability of any spontaneous Marx output is 10^{-6} or less. This relatively small timing jitter is due to a strong Marx triggering chain, which utilizes a high reliability, fast risetime primary trigger generator [7] that triggers nine Marx generators with $600\ \text{kV}$ output, that in turn trigger the 36 main Marxes. High reliability and low jitter together are crucial for a system like Z that often uses complicated and expensive loads (which could be destroyed by a mis-fire), and certain diagnostics (such as the multi-kilojoule, nanosecond duration laser backscatter) that require nanosecond precision of the load current timing to image fast features of load behavior. Small timing jitter and high reliability are generally competing requirements, and for that reason the Z pulsed power system relies heavily on robust triggering methods throughout.

The Marx generators charge water-insulated coaxial capacitors in $1.45\ \mu\text{s}$. The intermediate store capacitors lower the impedance and temporally compress the pulse. The intermediate store capacitors are discharged through laser triggered gas switches [8-12] that provide the final command-triggered stage in the pulse

compression process. The laser triggered gas switches developed for Z are the highest voltage nanosecond jitter gas switches yet developed. The Z laser triggered gas switches see a peak terminal voltage of 5.5 MV at 80 kV Marx charge voltage, and have a refurbishment lifetime in excess of 100 shots at full voltage. Figure 2 shows a sectional view of the Z laser triggered gas switch. After closure, the switch conducts a peak current of 600 kA with 80 kV Marx charge. Figure 3 shows laser triggered gas switch voltage and current on a typical operation with ± 80 kV Marx charge. The multichannel (rimfire) portion of the gas switch uses stainless steel electrodes; in that section of the switch, the current is carried in several (up to ten) parallel arc channels. The trigger gap electrodes are a copper-tungsten sintered material because there the entire switch current flows in a single channel, and stainless steel erodes rapidly under those conditions. The eroded trigger electrodes would cause an unacceptable increase in the switch pre-fire rate [9] due to electric field enhancement.

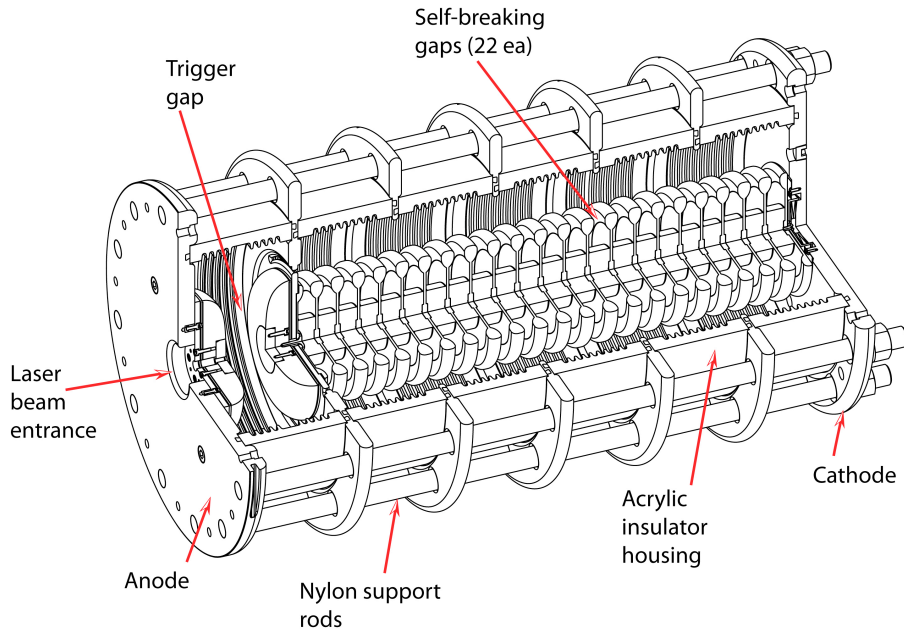


Figure 2. View of the laser triggered gas switch. The 46 mm trigger gap (left) is closed with plasma formed by 10-20 mJ of 266 nm laser light; the remainder of the switch then closes due to the subsequent over-voltage of the self-breaking gaps.

The measured standard deviation of the closure times for the 36 laser triggered gas switches has a median value 6.9 ns over a large number of shots; this is due almost solely to random fluctuations in run time. Consistent switch timing variations are removed by adjusting the trigger times. Triggering long-running switches sooner, and fast-running switches later effectively removes stable differences in run time, but cannot remove random timing fluctuations.

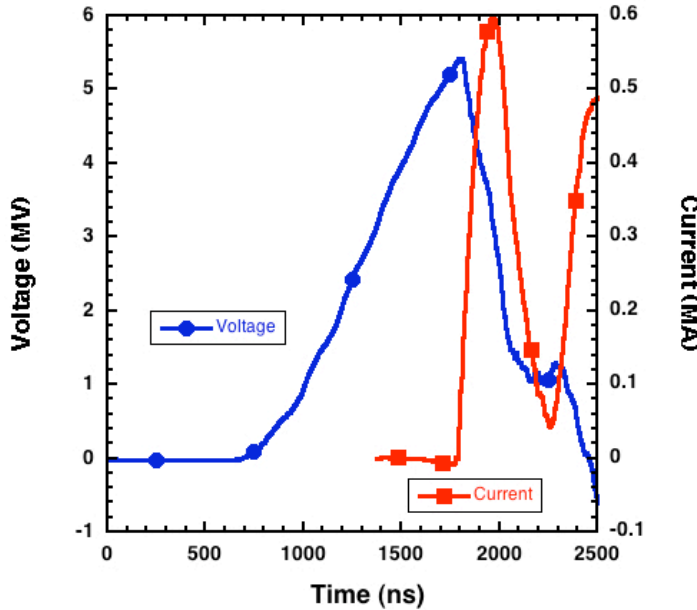


Figure 3. Gas switch voltage and current with 80 kV Marx charge.

The gas switch current charges another water-insulated capacitor. This capacitor is discharged through untriggered water switches [13-18]. Megavolt water switches allow relatively low inductance, and can have jitter that's a few percent of the charge time, especially for high voltages. At high voltages, the threshold for water streamer formation is crossed early in the charge time. This reduces the jitter due to variations in the statistical time during which the streamers in water launch from the surfaces [18]. The Z water switches see a peak terminal voltage of 2.6 MV with ± 80 kV Marx charge, and conduct 750 kA peak current after closure. The measured temporal variation of the module pulse times downstream of the water switches has a median value of 6.6 ns over a series of identical experiments. The water switches essentially do not contribute to the jitter of the pulse forming system (with the present gas switch jitter). If the gas

switch and water switch jitters are uncorrelated, the total jitter is the quadrature sum of the water switch and gas switch components, and so a water switch jitter 25% of the gas switch jitter is generally negligible.

The composite jitter of the combined pulses from the 36 modules is reduced because of averaging. If the individual module jitter is normally distributed, then the jitter of the summed pulse is reduced by \sqrt{n} , where n is the number of modules. The one-sigma jitter of the load current start time is 1.7 ns over a recent sequence of shots at 80 kV Marx charge voltage. Efforts are ongoing to reduce this value (concentrating on the laser triggered gas switch), while maintaining the required reliability.

The compressed pulse from each module flows on passive 6.4Ω water-insulated triplate transmission lines towards the center of the machine. The load energy flows through a plastic water-vacuum interface into vacuum (Figure 4). Vacuum flashover is an important consideration in the system design. Flashover of a surface in vacuum can be caused by formation of low-density gas or plasma near the insulator, which takes little energy [19], and can proceed quickly to a low impedance shunt path. Vacuum flashover [20-27] essentially affects system design through inductance (if the vacuum interface design is too conservative and therefore inductive) or performance limitations (if the design is too aggressive). The Z insulator stack is a conventional multi-stage 45-degree design [28], and operates reliably at an average peak axial electric field of 135 kV/cm [26]. The Z vacuum insulator stack has four parallel levels, with a large 1.65 meter radius, to reduce the inductance of the insulator.

The Z magnetically insulated transmission lines [29-34] carry current from the water-vacuum interface to the load region, shown in Figure 4. Magnetic insulation allows efficient power flow even at electric fields above the value at which electron emission occurs, typically 200 kV/cm for nanosecond pulses[35]. The Z magnetically insulated transmission lines operate at values well above 1 MV/cm, with a few percent (or less) of the total current in electron flow outside the load region. The electrons emitted from the cathode conductor are confined

by the magnetic field of the power flow, and drift towards the load at velocities much slower than the electromagnetic wave. During the current rise, which is the most important part of the current pulse, electrons are accelerated by the changing magnetic field, increasing their total energy, tending to drive some fraction of the electrons to the cathode in some cases [29].

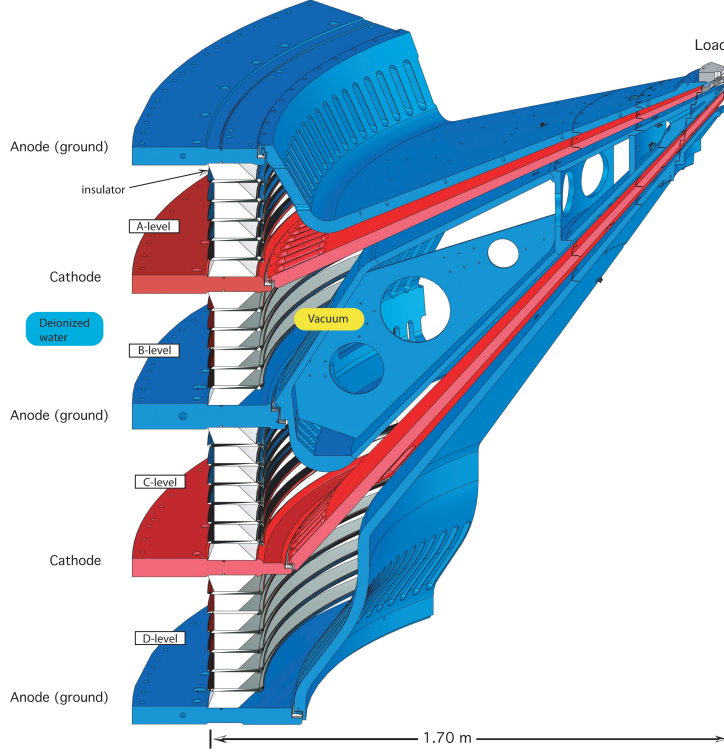


Figure 4. The water-vacuum interface and the magnetically insulated transmission lines feeding the load region.

At approximately 30 cm diameter, the four parallel transmission lines are combined into a single feed by a post-hole convolute structure [36-38]. The post-hole convolute has multiple localized magnetic nulls, where magnetic insulation is ineffective. It is believed that flowing electrons from the outer magnetically insulated regions (that have not returned to the cathode) are lost at the magnetic nulls, in addition to the locally generated electron flow loss.

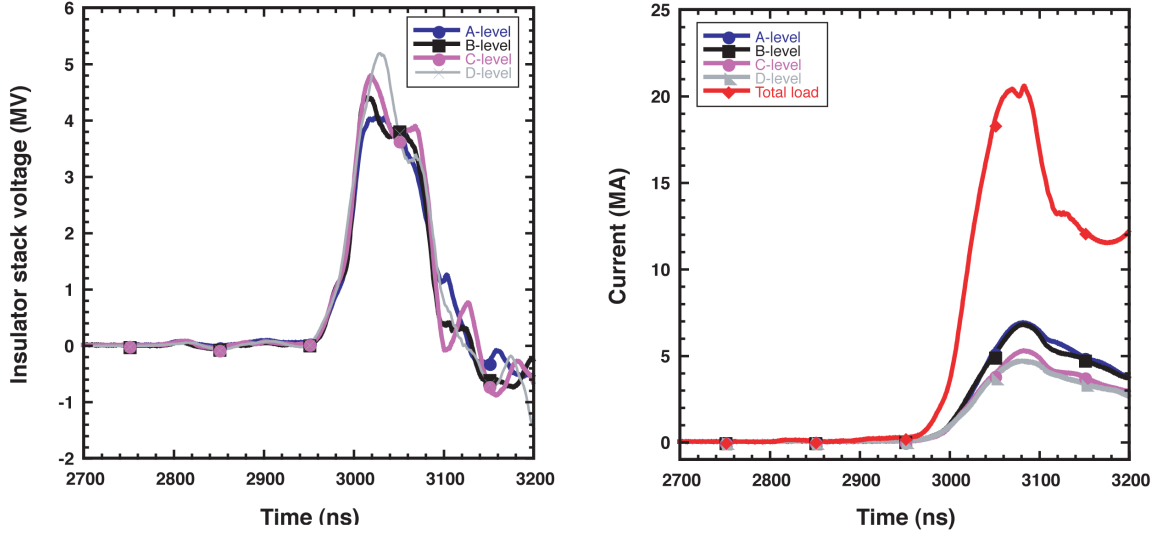


Figure 5. Measured insulator stack voltages, and currents on a single Z experiment. The upper stack level (A-level) sees lower voltage than the lower stack level (D-level) because of the lower inductance magnetically insulated transmission lines of the upper levels.

Applications

The Z driver is used to drive intense soft X-ray sources, drive high pressures in materials for isentropic equation of state measurements, and for launching flyer plate impacts, for determining points on the Hugoniot curve.

The Z data acquisition system records more than 600 waveforms on each test. Many of these are machine diagnostics, primarily used to determine the root causes of failures. Most of the Z digitizers can acquire long record lengths, and have 500 MHz analog bandwidth and sample at 500 ps per point. Z also has an extensive array of load diagnostics, from VISAR systems [39] to visible and X-ray streak and framing cameras, and time resolved spectrometers [40].

X-ray sources

High current z-pinches are well known as efficient converters of magnetic energy to X-radiation [41-43]. A cylindrical array of wires, a thin solid conductor, or a shell of low-pressure gas provides the material for carrying the megampere current. The magnetic pressure tends to implode the cylinder of plasma (increasing the inductance, and converting magnetic energy to kinetic energy). When the cylinder of plasma, moving at velocities up to 300 cm/μs,

stagnates on the power feed axis, the kinetic energy is thermalized. The z pinch essentially converts magnetic energy accumulated over the time to peak current (~ 80 ns in the case of Z), to thermal energy in a shorter time. The X-ray power is that case is higher than the driver power. The resulting energy is dissipated in a time scale determined by the effective physical dimensions of the plasma shell; as instabilities increase the radial thickness of the shell, the stagnation time increases and the peak radiated power decreases. A series on Z [44] recorded 3-4 nanosecond soft X-radiation full-width at half-maximum, with ~ 80 nanosecond implosion times and ~ 23 MA peak load current, from a 65 mm initial diameter tungsten wire array. The radiated power shown in Figure 6 was measured using a silicon diode array (24 meters from the z-pinch) normalized to a nickel bolometer measure of total energy [45]. The X-ray power measurement has a peak of 320 ± 30 TW, with a 2.9 ns full width at half maximum. The peak driver electrical power was 82 TW; the total radiated energy on that experiment was 2 MJ.

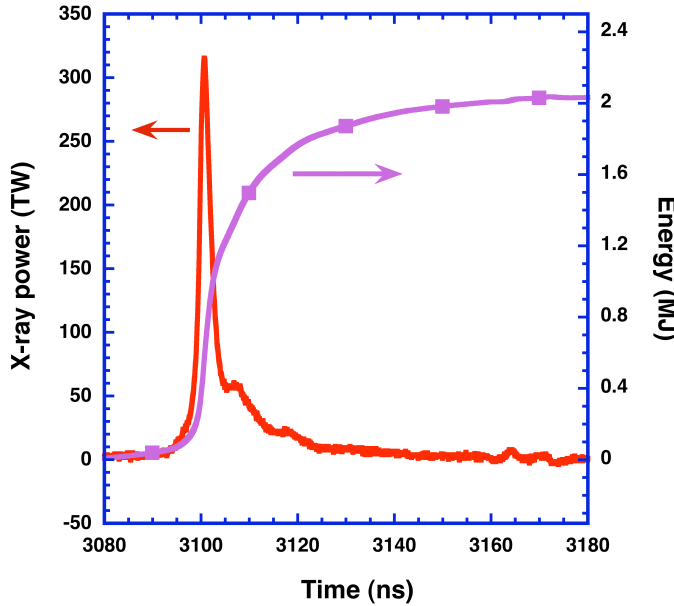


Figure 6. Total X-ray power and energy from a 23 MA tungsten wire array experiment. Power measured with apertured Si diodes 24 meters from the source.

Material equation of state studies

Currents in excess of 20 MA in cm width conductors create ~ 25 Megagauss magnetic fields. These magnetic fields create high pressures in conductors.

Because Z has 36 nominally independent modules, the system can be configured to drive temporal pressure profiles that do not induce shock waves in the mm thickness samples used. Shock free measurements allow mapping sections of the Hugoniot curve for a material. Z has a unique capability to provide multi-megabar ramped compression waves, by delivering tailored current time histories. Because the sound speed generally increases with pressure, with increasing pressure there will generally be a point of shock formation somewhere in an infinitely thick sample. However, with a finite sample thickness, it is possible to prevent shock formation by limiting the rise time of the applied loading waveform. From the simple conceptual view of Figure 7, it is clear that the rise time should be constrained by

$$\tau_r \geq x_L \left[\frac{1}{C_{\min}} - \frac{1}{C_{\max}} \right],$$

where c_{\min} and c_{\max} are the minimum and maximum pressure wave sound speeds, respectively, x_L is the Lagrangian thickness parameter, and τ_r is the pulse rise time. The minimum thickness of the sample is limited by reverberation of waves reflected from the accelerated surface [5]. In practice, the optimum pulse shape is determined using hydrodynamic simulations. Figure 7 shows current in a machine configuration for fast current rise times (short pulse) and a tailored current risetime designed to prevent shock formation in a material sample. The Z system has been used with such shaped pulses to measure the properties of a variety different materials [4, 5].

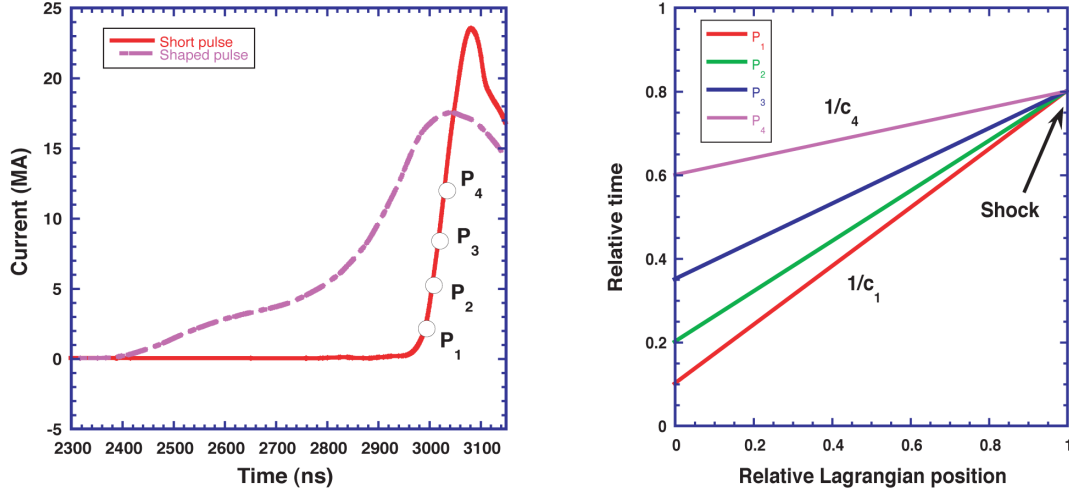


Figure 7. Shock formation in a sample where the sound speed (c_i) increases with pressure (P_i). Representative points in a fast-rising current waveform (short pulse) are shown, along with a conceptual view of shock formation. A longer rise time current pulse (shaped pulse) prevents shock formation.

Shock mitigation is also important in flyer plate experiments, where a single point on the Hugoniot curve is determined by impacting a flyer on a stationary material sample. In those experiments, it is important to have the flyer plate in a known state at impact. For those applications as well, pulse shaping is used to prevent shock formation in the flyer plate. A flyer plate method was used to measure properties of liquid deuterium at high pressures [46]. Flyer plates roughly mm thick have been accelerated to 40 km/sec by 1200 Tesla magnetic fields [47], while remaining partially solid. These velocities substantially exceed those available from gas guns, for example.

Conclusions

The Z system is a low impedance, fast pulsed, high current driver. Delivering more than 20 MA in 85 ns to a single load allows measurements on plasma at high temperatures and materials at high pressures. As a reusable laboratory X-ray source, Z is unique for providing more than two megajoules of blackbody radiation, with more than 300 terawatts of peak power. As a source of intense magnetic field and pressures, Z is used to map equation of state characteristics of

materials at megabar pressures. By its position as the only facility of its kind, Z is also a platform for developing components for megavolt pulsed power systems.

Acknowledgments

Z is a large and complicated system, and functions well due to a talented and dedicated operations team. This group responds to challenges with speed and energy. Among the hard-working group that allows the system to operate, the authors would like to thank Tom Avila, Mike Baremore, Terrence Bock, Alan Carlson, Ray Chavez, Guy Coombs, Josh Cordova, Mark Dudley, Geoff Gatewood, Jeff Georgeson, Nibby Grille, Dale Hodgson, Al Jojola, Andy Kipp, Barbara Lewis, Pat Lake, John Lott, Jerry Mills, Jim Moore, Dan Nielson, Linda Neilson-Weber, Dana Pariza, Don Petmecky, Steve Ploor, Charlie Robinson, Gene Ross, Scott Roznowski, Larry Ruggles, Johnny Santillanes, Tom Schweitzer, Hans Seamen, Dawn Thomas, Hans Wagoner, David Wenger, and Shawn White.

References

- ¹ F. L. Cochran, J. Davis, and A. L. Velikovich, "Stability and radiative performance of structured Z-pinch loads imploded on high-current pulsed power generators" *Physics of Plasmas* 2, 2765 (1995).
- ² M. G. Haines and M. Coppins, "Universal diagram for regimes of Z-pinch stability" *Physical Review Letters* 66, 1462 (1991).
- ³ M. G. Haines, S. V. Lebedev, J. P. Chittenden, *et al.*, "The past, present, and future of Z pinches" *Phys. Plasmas* 7, 1672 (2000).
- ⁴ M. D. Knudson, R. W. Lemke, D. B. Hayes, *et al.*, "Near-absolute Hugoniot measurements in aluminum to 500 GPa using a magnetically accelerated flyer plate technique" *Journal of Applied Physics* 94, 4420 (2003).
- ⁵ J.-P. Davis, C. Deeney, M. D. Knudson, *et al.*, "Magnetically driven isentropic compression to multimegabar pressures using shaped current pulses on the Z accelerator" *Physics of Plasmas* 12, 056310 (2005).
- ⁶ R. A. Fitch, "Marx- and Marx-like- high voltage generators" *IEEE Trans. Nucl. Sci.* NS-18, 190 (1971).
- ⁷ M. E. Savage and B. S. Stoltzfus, "High reliability low jitter 80 kV pulse generator" *Phys. Rev. ST Accel. Beams* 12, 080401 (2009).

8 D. R. Humphreys, K. J. Penn, J. S. Cap, *et al.*, 5th IEEE International Pulsed Power Conference, Arlington, VA, 1985, (IEEE Press) p. 262.

9 K. R. LeChien, M. E. Savage, V. Anaya, *et al.*, "Development of a 5.4 MV laser triggered gas switch for multimodule, multimegampere pulsed power drivers" Physical Review Special Topics - Accelerators and Beams 11, 060402 (2008).

10 H. Li, J. Deng, W. Xie, *et al.*, "The delay and jitter characteristics of laser-triggered multistage switch: a parametric study" IEEE Trans. on Plasma Science 35, 1787 (2007).

11 J. R. Woodworth, R. G. Adams, and C. A. Frost, "UV-laser triggering of 2.8-Megavolt gas switches" IEEE Trans. on Plas. Sci. PS-10, 257 (1982).

12 J. R. Woodworth, P. J. Hargis, L. C. Pitchford, *et al.*, "Laser triggering of a 500-kV gas-filled switch: A parametric study" J. Appl. Phys. 56, 1382 (1984).

13 J. M. Elizondo, J. Corley, K. W. Struve, *et al.*, Pulsed Power Conference, 2003. Digest of Technical Papers. PPC-2003. 14th IEEE International, 2003, 171.

14 D. L. Johnson, J. P. VanDevender, and T. H. Martin, "High power density water dielectric switching" IEEE Trans. Plasma Sci. PS-8, 204 (1980).

15 J. Lehr, J. Maenchen, J. Woodworth, *et al.*, 14th International Pulsed Power Conference, Dallas, TX, 2003, (IEEE Press, Piscataway, NJ) p. 609.

16 J. P. VanDevender, "The resistive phase of a high-voltage water spark" J. Appl. Phys. 49, 2616 (1978).

17 J. P. VanDevender and T. H. Martin, "Untriggered water switching" IEEE Trans. Nucl. Sci. NS-22, 979 (1975).

18 J. R. Woodworth, J. M. Lehr, J. Elizondo-Decanini, *et al.*, "Optical and pressure diagnostics of 4-MV water switches in the Z-20 test facility" IEEE Trans. Plasma Sci. 32, 1778 (2004).

19 I. D. Smith, "Induction voltage adders and the induction accelerator family" Physical Review Special Topics - Accelerators and Beams 7, 064801 (2004).

20 R. A. Anderson, "Mechanism of fast surface flashover in vacuum" Appl. Phys. Lett. 24, 54 (1974).

21 K. D. Bergeron, "Theory of the secondary electron avalanche at electrically stressed insulator-vacuum interfaces" J. Appl. Phys. 48, 3073 (1977).

22 E. W. Gray, "Vacuum surface flashover: A high-pressure phenomenon" Journal of Applied Physics 58, 132 (1985).

23 J. C. Martin, Atomic weapons research establishment Internal Report, "Fast pulse vacuum flashover", SSWA/JCM/713/157, 1971

²⁴ H. C. Miller, "Flashover of insulators in vacuum: Review of the phenomena and techniques to improve holdoff voltage" IEEE Trans. on Electrical Insulation 28, 512 (1993).

²⁵ O. Milton, "Pulsed flashover of insulators in vacuum" IEEE Trans. Electrical Insulation EI-7, 9 (1972).

²⁶ W. A. Stygar, H. C. Ives, T. C. Wagoner, *et al.*, "Flashover of a vacuum-insulator interface: A statistical model" Physical Review Special Topics - Accelerators and Beams 7, 070401 (2004).

²⁷ W. A. Stygar, J. A. Lott, T. C. Wagoner, *et al.*, "Improved design of a high-voltage vacuum-insulator interface" Physical Review Special Topics - Accelerators and Beams 8, 050401 (2005).

²⁸ I. D. Smith, "Flashover of vacuum interfaces with many stages and large transit times" IEEE Trans. on Plasma Science 25, 293 (1997).

²⁹ J. P. Martin, M. E. Savage, T. D. Pointon, *et al.*, "Tailoring of electron flow in magnetically insulated transmission lines" Phys. Rev. ST-AB 12, 1 (2009).

³⁰ C. W. Mendel, Jr. and S. E. Rosenthal, "Modeling magnetically insulated devices using flow impedance" Phys. Plasmas 2, 1332 (1995).

³¹ C. W. Mendel, Jr. and D. B. Seidel, "Flow impedance in a uniform magnetically insulated transmission line" Physics of Plasmas 6, 4791 (1999).

³² C. W. Mendel, Jr., D. B. Seidel, and S. E. Rosenthal, "A simple theory of magnetic insulation from basic physical considerations" Laser and Particle Beams 1, 311 (1983).

³³ W. A. Stygar, P. A. Corcoran, H. C. Ives, *et al.*, "55-TW magnetically insulated transmission-line system: Design, simulations, and performance" Physical Review Special Topics - Accelerators and Beams 12, 120401 (2009).

³⁴ W. A. Stygar, T. C. Wagoner, H. C. Ives, *et al.*, "Analytic model of a magnetically insulated transmission line with collisional flow electrons" Physical Review Special Topics - Accelerators and Beams 9, 090401 (2006).

³⁵ G. E. Vogtlin and J. E. Vernazza, 7th IEEE Pulsed Power Conference, Monterey, Ca, 1989, (IEEE Press) p. 808.

³⁶ T. D. Pointon, W. L. Langston, and M. E. Savage, Pulsed Power Plasma Science 2007, Albuquerque, NM, 2007.

³⁷ T. D. Pointon, W. A. Stygar, R. B. Spielman, *et al.*, "Particle-in-cell simulations of electron flow in the post-hole convolute of the Z accelerator" Physics of Plasmas 8, 4534 (2001).

³⁸ D. V. Rose, D. R. Welch, T. P. Hughes, *et al.*, "Plasma evolution and dynamics in

high-power vacuum-transmission-line post-hole convolutes" Physical Review Special Topics - Accelerators and Beams 11, 060401 (2008).

³⁹ L. M. Barker and R. E. Hollenbach, "Laser interferometer for measuring high velocities of any reflecting surface" Journal of Applied Physics 43, 4669 (1972).

⁴⁰ T. J. Nash, M. S. Derzon, G. A. Chandler, *et al.*, "Diagnostics on Z (invited)" Rev. Sci. Instr. 72, 1167 (2001).

⁴¹ C. Deeney, M. R. Douglas, R. B. Spielman, *et al.*, "Enhancement of X-Ray Power from a Z Pinch Using Nested-Wire Arrays" Physical Review Letters 81, 4883 (1998).

⁴² C. Deeney, D. L. Peterson, R. B. Spielman, *et al.*, "Optimization of power density by decreasing the length of tungsten wire array Z pinches" Physics of Plasmas 5, 2605 (1998).

⁴³ R. B. Spielman, C. Deeney, G. A. Chandler, *et al.*, "Tungsten wire-array Z-pinch experiments at 200 TW and 2 MJ" Physics of Plasmas 5, 2105 (1998).

⁴⁴ Facility I Series - Shot Series Summary 10/7/2009, M. Jones, 2009), p. Sandia National Laboratories Internal Memorandum.

⁴⁵ H. C. Ives, W. A. Stygar, D. L. Fehl, *et al.*, "Measurement of the energy and power radiated by a pulsed blackbody x-ray source" Physical Review Special Topics - Accelerators and Beams 9, 110401 (2006).

⁴⁶ M. D. Knudson, D. L. Hanson, J. E. Bailey, *et al.*, "Equation of State Measurements in Liquid Deuterium to 70 GPa" Physical Review Letters 87, 225501 (2001).

⁴⁷ R. Lemke, M. Knudson, and J.-P. Davis, "Magnetically driven hypervelocity launch capability at the Sandia Z accelerator" 11th Hypervelocity Impact Symposium, Freiburg, Germany,